ELSEVIER

Tectonophysics 357 (2002) 137–158

TECTONOPHYSICS

www.elsevier.com/locate/tecto

Structural inheritance and cenozoic stress fields in the Jura fold-and-thrust belt (France)

C. Homberg [a,*], F. Bergerat [a], Y. Philippe [b], O. Lacombe [a], J. Angelier [a]

[a] *Université Pierre et Marie Curie, Laboratoire de Tectonique, UMR 7072-CNRS, Case 129, 4 Place Jussieu, 75252 Paris Cedex 05, France*

[b] *TotalFinaElf E&P Inc, 800 Gessner, Suite 700, Houston, TX 77024 USA*

Received 16 May 2000; accepted 12 December 2001

Abstract

Based on an analysis of 8000 minor fault-slip data in the Jura Mountains (France), we discuss the influence of pre-existing discontinuities on the development of fold-and-thrust belts. We present palinspastic maps showing the stress fields and active faults during the Cenozoic pre-orogenic events in the Jura belt prior to the main Late Miocene fold-and-thrust tectonics. During the Eocene, a N–S strike-slip regime produced a few NNE–SSW sub-vertical strike-slip faults in the central external Jura and a few E–W reverse faults in the eastern Jura near the future frontal thrust. During the Oligocene, an average WNW–ESE extension, with irregular stress trajectories, resulted in normal faulting along N–S to NE–SW trends in the external part of the belt, WNW–ESE trends along the future northern and northeastern frontal thrust, and NW–SE trends in the internal Jura. The Late Miocene tectonics began with a strike-slip regime with a fan-shaped compressional trajectory. It was followed by a stress field with similar stress direction, but local σ_2/σ_3 stress permutation resulted in strike-slip regime domains contrasting with reverse regime domains. Stress deflections and permutations occurred near inherited cover and basement discontinuities. Major deformation zones, like the Jura frontal thrust onto the foreland, the thrust of the internal central Jura onto the external Jura, and the narrow deformation bands within the flat-lying plateaus formed close to the inherited faults. The structural style of the Jura belt thus partly mimics the pre-orogenic fault pattern. Stress deflections point to the pre-orogenic faults, express the indentation process of the Jura by its hinterland, and highlight successive slip events along major faults during the fold-and-thrust tectonics. This case study illustrates the relevance of minor fault-slip studies for characterizing both the pre-orogenic tectonics and the kinematics of the deformation.

Keywords: Pre-existing faults; Inheritance; Cenozoic stresses; Jura Mountains; Fold-and-thrust belt; Alpine tectonics; Oligocene rifting; Stress deflections

1. Introduction

Physical models (e.g., Davis et al., 1983; Malavieille, 1984; Davis and Engelder, 1985; Huiqi et al., 1992) have led to a better understanding of some overall mechanical aspects of fold-and-thrust belts

* Corresponding author. Tel.: +33-1-44-27-52-74; fax: +33-1-44-27-50-85.

E-mail address: catherine.homberg@lgs.jussieu.fr (C. Homberg).

0040-1951/02/$ - see front matter © 2002 Elsevier Science B.V. All rights reserved.
PII: S0040-1951(02)00366-9

development. They have provided significant insight into the influence of the frictional properties of the basal décollement and the prism thickness on the structural characteristics of fold-and-thrust belts. In these purely homogeneous brittle models, foreland-verging thrusts (and associated folds), with variable degrees of back-thrusts, typically form in a piggy-back sequence with a uniform spacing. Most of the active deformation occurs along the most foreland-ward thrust. As suggested by additional analog and numerical experiments (e.g., Ballard et al., 1987; Marshak et al., 1992; Sassi et al., 1993; Letouzey et al., 1995; Philippe et al., 1996; Vanbrabant et al., 1999), other structural and rheological parameters, like ductile materials within and at the base of the sedimentary pile, irregularities in the basal décollement (especially variation in thickness, lateral pinch outs, fault offsets and flexures) are crucial for the structural style of the belt. Of particular importance to this respect are pre-orogenic faults and foreland obstacles.

Pre-existing faults are common in fold-and-thrust belts. For example, many large fractures have developed in passive margins prior to belt development. However, attempts to quantify the influence of pre-orogenic deformation in the development of natural fold-and-thrust belts face the difficulty of recognizing the pre-orogenic faults inside deformed belts. Indeed, ancient faults are often reactivated with a larger offset, so that the earlier slip is no longer identifiable and lateral variations of layer thickness or of lithology which may be related to early tectonic events are generally difficult to interpret unambiguously.

Our goal is to illustrate the relevance of minor fault analysis for the recognition of pre-orogenic tectonics and to discuss the role of inherited discontinuities in fold-and-thrust belt development through the case example of the Jura Mountains. The Jura is a thin-skin fold-and-thrust belt, shortened by about 30 km (Laubscher, 1961; Guellec et al., 1990; Philippe et al., 1996; Burkhard and Sommaruga, 1998) and displaced northwestward above the plastic Triassic evaporites during Alpine tectogenesis (Buxtorf, 1907; Michel et al., 1953; Laubscher, 1961; Jordan, 1992). Deformation was active from about 10 to 5 Ma ago and is referred to as the "Jura Phase" or the Late Miocene tectonics (for a review, see Burkhard, 1990; Laubscher, 1992). Early deformation in the Jura Mountains has been locally identified (e.g., Mathis, 1974; Laubscher, 1972, 1986; Chauve et al., 1988), but the detailed fracture pattern and corresponding stress fields have not been considered for the whole Jura Mountains. In addition, origin of pre-orogenic deformation in the Jura and in neighboring areas is controversial (Sopena and Soulas, 1973; Illies, 1975; Buchner, 1981; Bergerat and Geyssant, 1987; Lacombe and Angelier, 1993; Homberg et al., 1994).

First, we discuss the relevance of minor fault analysis to the recognition of pre-orogenic events. Secondly, we present the results of an extensive minor fault analysis in the Jura Mountains. Faulting and stress fields during the Paleogene pre-orogenic events are described. We then reconstruct the stress fields that prevailed during the Jura folding and thrusting (Late Miocene tectonics) and discuss how the stress deflections reflect the kinematic evolution of the belt and its pre-orogenic structures. Finally, we present a structural evolutionary model of the Jura during the Cenozoic and discuss the main thrust tectonics, devoting particular attention to the influence of inherited structures on the structural style of the belt.

2. What does minor faulting tell about pre-orogenic tectonics?

2.1. Recognition of pre-orogenic tectonics

Pre-orogenic faults are often difficult to identify as they are typically involved in subsequent tectonics. They are commonly reactivated with a larger offset or themselves re-deformed. However, small-scale brittle deformation (faults with millimetric to decimetric displacement, tension gashes with millimetric to centimetric opening, stylolites), often escape subsequent deformation. Previous slip on minor faults is often preserved because minor slip associated with subsequent tectonic episodes occurs on newly developed fracture surfaces. A few faults may be reactivated, however. In ideal cases, the successive events of slip can be identified, thus revealing superposed deformations (Fig. 1). Furthermore, minor faults and associated brittle features are generally abundant and well represented despite erosion. Extensive data can thus be collected.

Analyses of minor brittle structures in various tectonic contexts have shown that they reliably reflect

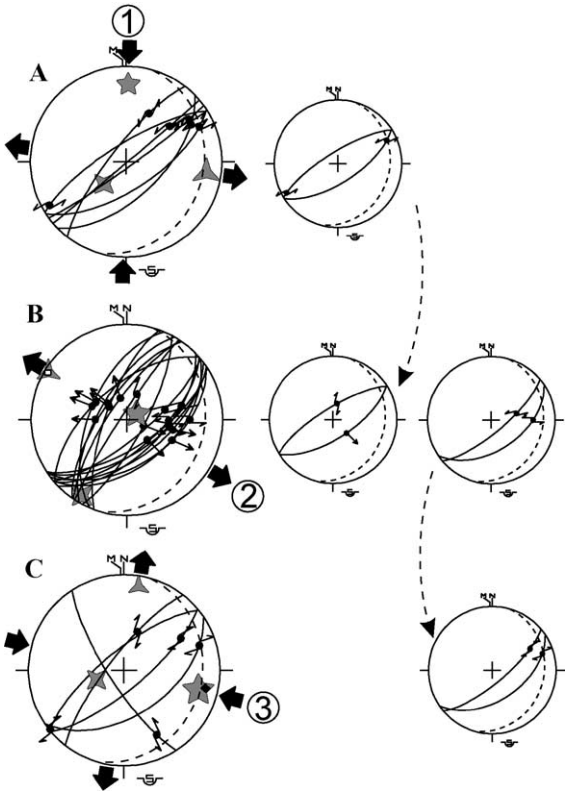

Fig. 1. Identification of the previous tectonics from minor fault analysis and stress calculation. Mechanical incompatibilities in the fault population collected in a 100-m long outcrop near the Euthe Pinçée (5 in Fig. 3) led to distinguish three fault subsets, (A), (B), and (C) (lower hemisphere, equal-area projection). Stress states responsible of each subset are shown. Relative chronologies (dotted long arrows) between superposed striae on fault planes (right diagrams) allow establishment of stress state succession (encircled numbers). Continuous lines: fault planes. Slickenside lineations in dots with double arrows for strike-slip motion, outward-directed single arrow for normal motion, and inward-directed single arrow for reverse motion. Black lozenges: stylolites. Dashed lines: bedding planes. Gray stars with 5, 4, 3 arms: σ_1, σ_2, and σ_3, respectively. Convergent and divergent large black arrows show directions of σ_1 and σ_3, respectively.

the large-scale regional deformation (e.g., Mattauer and Mercier, 1980; Angelier et al., 1982; Le Pichon et al., 1988). Early tectonic events can be inferred from a mechanical analysis of the data collected on minor faults. Because each of the successive tectonic events was generally characterized by its own stress field, polyphase tectonism can be inferred from the mechanical inconsistencies in fault population (Fig. 1) especially verified through the calculation of the stress state responsible for the minor slips (inversion process, see below). Relative chronologies (e.g., cross-cutting relationships, superposition of striations on fault planes, etc.) help to classify any heterogeneous fault population into homogeneous subsets.

Numerous 3-D reconstructions of present-day stresses (e.g., Cornet and Burlet, 1992; Brudy et al., 1997) indicate that stresses in the crust generally follow the model of Anderson (1942), in which one principal stress is vertical and corresponds to the lithostatic pressure. Hence, pre-orogenic stress states are inferred if none of the principal stresses is vertical, and two principal stresses lie within the bedding plan (Fig. 2). Such a geometrical relationship means that these two principal stresses were horizontal before tilting (the third one being vertical). In other words, stresses are in agreement with the Andersonian model considering that the corresponding faults formed before tilting. Because folding is generally acquired during the orogenic event, pre-folding stress states thus express pre-orogenic events, especially if they do not fit the orogenic stress field. Stress deflections resulting in principal stresses at significant angles to the horizontal may exist, like those due to folding in an anisotropic layered medium. However, because such deflected stress states very unlikely exhibit two principal stresses lying in the bedding plane, they

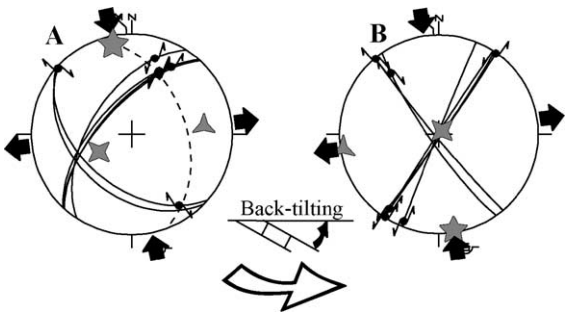

Fig. 2. Age of faulting relative to folding. Example of Eocene minor fault-slip data (see Section 4) in a site of measurement in the internal Jura. Minor faults (and related stress state) are shown in their present-day attitudes (A) and after rotation around the local bed strike of the amount of tilting (back-tilting) (B). Stress state is in agreement with the Andersonian model (i.e., one principal stress vertical) when faults are considered in their back-tilted attitude. Faults thus developed before folding. Same symbols as in Fig. 1.

cannot be confused with pre-folding stress states. Systematic examination of the accordance of the calculated stress states with the Andersonian model thus establishes the age of faulting relative to folding and allows recognition of pre-orogenic faults. The authors consider that a minimum 20° bed tilting is necessary to reliably establish the faulting-before-folding chronology.

2.2. Stress field and large-scale faulting

The stress state responsible for each homogeneous fault subset is calculated through an inversion process, using the INVDIR method of Angelier (1990). Fault-slip vectors incompatible with the mean calculated stress state are identified from their individual misfit with the calculated shear stress, discarded, and a new inversion is performed. This procedure is followed until a satisfactory agreement between the fault-slip vectors and the calculated stress state is obtained. Discarded faults are tested for mechanical compatibility with other fault subsets, or are used to form another homogeneous subset. An automatic classification procedure may also be used on the total fault population (Angelier and Manoussis, 1980; Angelier, 1984). The inversion process allows the determination of the direction of the three principal stresses σ_1, σ_2, and σ_3 ($\sigma_1>\sigma_2>\sigma_3$, compression positive) and of a ratio Φ between their magnitude, with $\Phi=(\sigma_2-\sigma_3)/(\sigma_1-\sigma_3)$. If faults are variable in orientation and if conjugate sets exist, the accuracy of stress plunge and direction is better than 10°. The fault population has

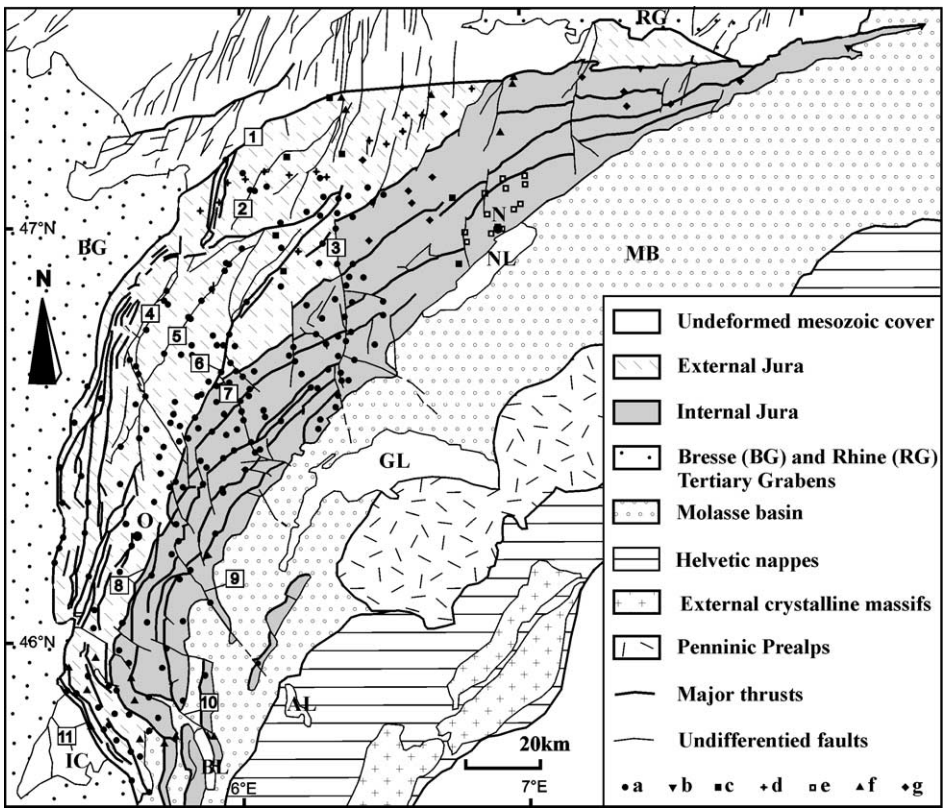

Fig. 3. Structural map of the Jura fold-and-thrust belt and sites of measurement. 1: Bisontin Faisceau; 2: Mamirolle Pinçée; 3: Pontarlier Fault; 4: Pupillin Pinçée; 5: Euthe Pinçée; 6: Syam Faisceau; 7: Morez Fault; 8: Oyonnax Thrust; 9: Vuache Fault; 10: Culoz-Pont d'Ain Fault; 11: Bugey Faisceau. IC: Ile Crémieu. Molasse Basin. AL, BL, GL, NL: Annecy, Bourget, Geneva, Neuchâtel lakes. Cities: Oyonnax (O) and Neuchâtel (N). Sites of paleo-stress determination from various sources. a: Homberg, 1997; b: Bergerat, 1987; c: Tschanz, 1990; d: Lacombe, 1992; e: Tschanz and Sommarugua, 1993; f: Philippe, 1995; g: Choi, 1996.

to be collected in a volume where the stresses can be considered as homogeneous. Attention must be paid to areas characterized by discontinuities in the stress field (e.g., near large faults).

Stress trajectories of pre-orogenic phases are reconstructed by associating similar local stress states and taking relative chronologies into account. However, it is important to keep in mind that different directions of stresses or superposed stress states do not necessarily indicate polyphase tectonics. Stresses may show local deflections (e.g., Rawnsley et al., 1992; Rebaï et al., 1992; Lacombe et al., 1993; Petit and Mattauer, 1995; Homberg et al., 1997; Kattenhorn et al., 2000) or rapidly vary in a locality (e.g., Hauksson, 1994; Homberg et al., 1999; Bergerat and Angelier, 2000; Homberg, 2000) even if the overall state of stresses is homogeneous. Relative chronologies are the most factor in assigning deviated stress states to otherwise homogeneous stress field.

Major pre-orogenic faults may be difficult to identify through classical marker offsets. Careful examination of fault surfaces may reveal superposed striae, where the early slip is compatible with one of the pre-orogenic stress fields inferred from minor fault analysis. The spatial distribution of minor faults provides further evidence of pre-orogenic large-scale faults. Indeed, in active fault zones, most small shocks occur close to a large fault. If this distribution is representative of the long-term behavior of faults, minor faults should be concentrated close to major faults. Major pre-orogenic faults are thus inferred where minor faults exhibit a swarm distribution.

3. Data and results in the Jura Mountains

Over 8000 fault-slip data were collected from 200 localities in the Bajocian to Barremian limestone

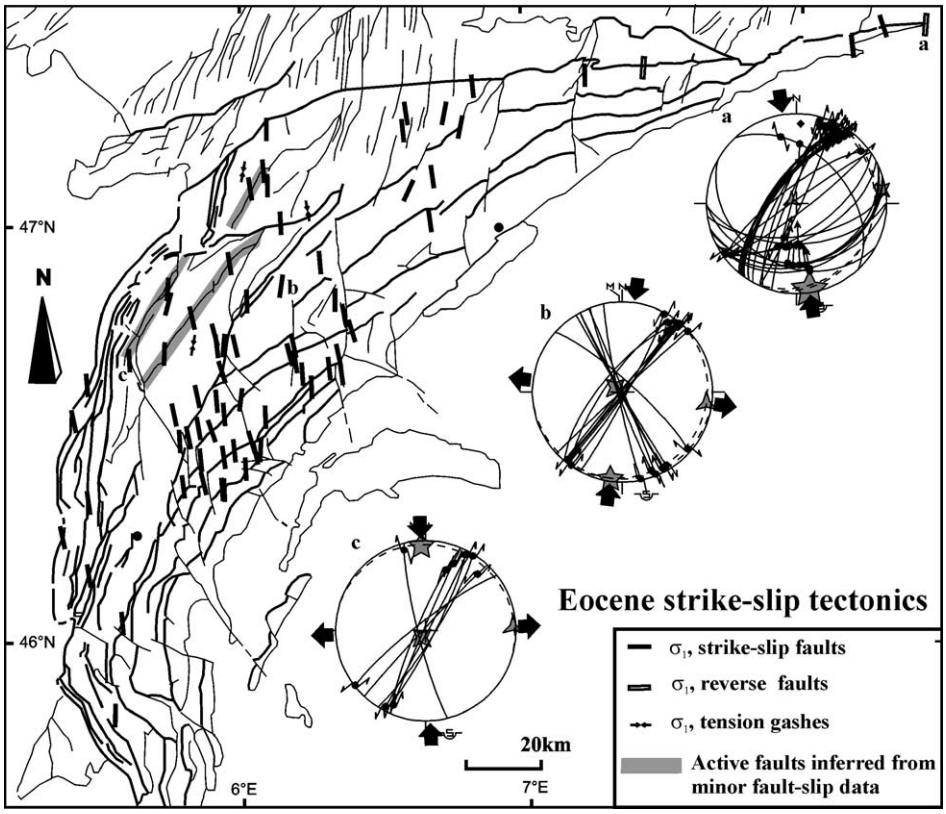

Fig. 4. Stress field and active faults during the Eocene compression. Examples of fault-slip data are shown for three sites. Same symbols as in Fig. 1.

strata of the Jura Mountains (Fig. 3). A total of 437 stress states were determined based on the fault-slip inversion method mentioned above. The available paleomagnetic data (Eldredge et al., 1985; Gehring et al., 1991) indicate that horizontal block rotations in the Jura did not exceed 10°. Since such rotations remain minor, the fault-slip inversion carried out in the present-day configuration reliably reflects the true paleo-stress orientation. Stylolitic peaks and tension gashes were also measured. In a few sites, they revealed a stress state that could not be recognized based on the sole inversion of minor fault-slips. Where such brittle structures were numerous, a statistical mean of the direction of stylolitic peaks and of the normal to tension gashes was calculated, in order to determine the direction of σ_1 and σ_3, respectively.

In most sites, the fault population was polyphase, indicating that several stress states have successively occurred. Comparison between the local stress successions in each site led to the identification of three main tectonic events and two minor ones. The last main event is characterized by a fan-shaped compression, perpendicular to major thrusts and folds, with a mean NW–SE direction. It includes syn- and post-folding stress sates and accounts for a very large proportion (86%) of the collected minor fault-slips. This event corresponds to the Alpine tectonics that occurred in the Jura during Late Miocene (Jura Phase). Fourteen percent of minor fault-slips does not fit this main stress field. They correspond to a first N–S compression (Fig. 4) defining a strike-slip regime (8% of the data), followed by a WNW–ESE extension (Fig. 5; 3% of the data) and a minor NE–

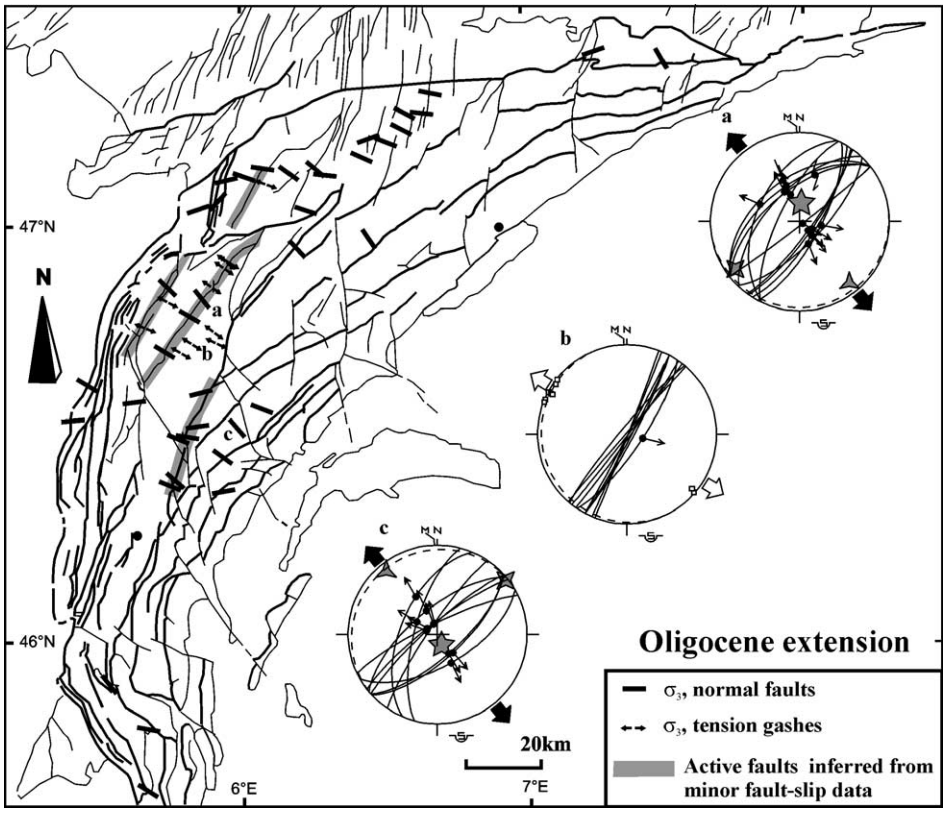

Fig. 5. Stress field and active faults during the Oligocene extension. Examples of fault-slip data are shown for three sites. Same symbols as in Fig. 1. For diagram (b), brittle structures are tension gashes (thin lines for planes and squares for poles) and one normal fault (thin line with arrow).

SW extension (Fig. 6; 2% of the data). In folded areas, these three stress states were clearly identified as predating folding (Fig. 2). Relative chronology criteria between brittle structures confirm that they predate the Jura Phase (Fig. 1) and thus correspond to pre-orogenic events. One percent of the fault-slips indicates a late WNW–ESE extension, which is not discussed here as it postdates folding and thus corresponds to post-orogenic deformation. Because Cenozoic formations are scarce in the Jura Mountains, dating of the pre-orogenic events requires to extrapolate the timing established in the neighboring areas. As discussed in the next section, the N–S strike-slip tectonics is thought to correspond to the expression of the so-called Pyrenean orogeny (early alpine tectonics) in the Jura Mountains and the WNW–ESE extensional tectonics to the west-European rifting at Eocene and Oligocene times, respectively.

4. The Cenozoic pre-orogenic tectonics in the Jura

4.1. The Eocene strike-slip tectonics

A N–S compression, defining a strike-slip regime, was recognized in 76 sites (Fig. 4). In 25 sites, significant bed tilting established that the N–S compression predates folding (Fig. 2). Associated brittle structures are N20°E to N50°E sinistral faults, N120°E to N170°E dextral ones, sub-meridian vertical tension gashes and sub-horizontal N–S stylolitic peaks. In the eastern Jura limb, a few minor E–W reverse faults defining a N–S pure compressive regime have been related to this early deformation (Bergerat and Geyssant, 1987) through relative chronologies that indicate they predate Oligocene normal faulting (see below).

The youngest formations affected by the N–S strike-slip compression are Hauterivian in age. This

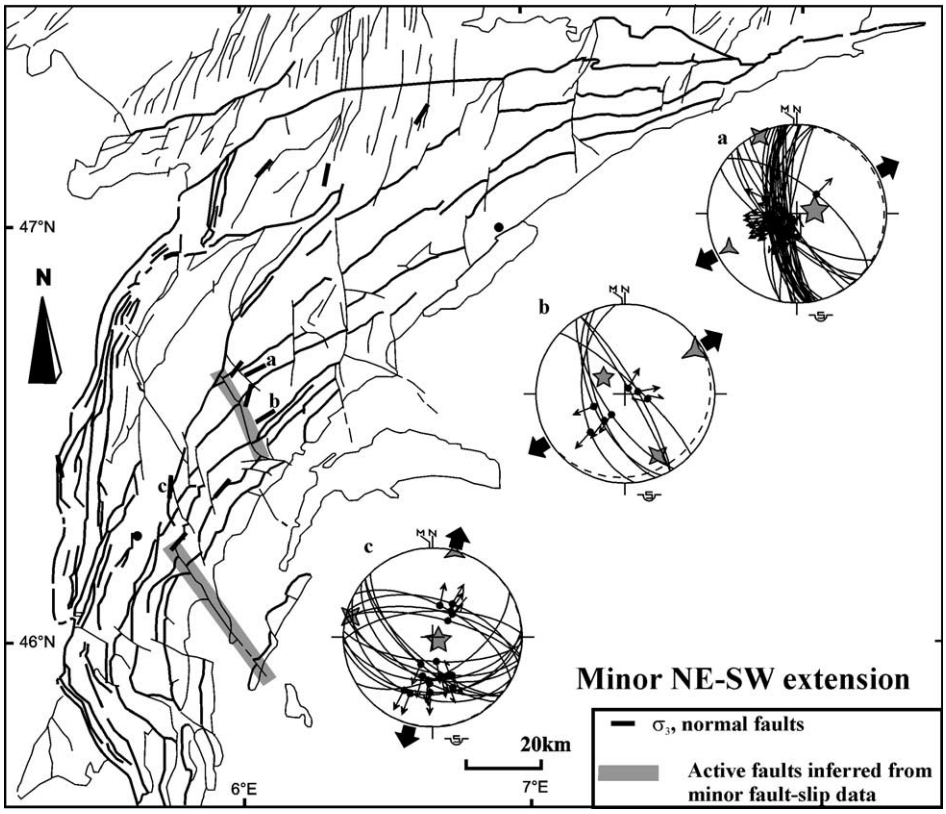

Fig. 6. Stress field and active faults during the minor NE–SW extension. Examples of fault-slip data are shown for three sites. Same symbols as in Fig. 1.

early phase thus postdates Early Cretaceous. In 15 sites, superposed striae on fault surfaces and cross-cutting relationships between brittle structures indicate that the N–S compression is the earliest compressive tectonic event. NE–SW and NW–SE fault planes often exhibit two sets of slickenside lineations (Fig. 1). The first slip on the NE–SW and NW–SE planes was sinistral and dextral, respectively, and corresponds to the N–S compression. The second ones are respectively dextral and sinistral and occurred during the Late Miocene orogenic phase (see Fig. 7). Late sinistral slip on the N–S tension gashes during the Late Miocene Phase confirms that the N–S compression predates the main fold-and-thrust Jura tectonics. Some NE–SW planes bear an additional normal slip, corresponding to a WNW–ESE extension (Fig. 1). In three sites, these dip-slip striae clearly cross-cut the sinistral slip, indicating that the WNW–ESE extension, thought to be Oligocene in age, postdates the N–S compression.

The strike-slip N–S compression has probably started in the Jura Mountains at Early Eocene and persisted until Early Oligocene. For simplicity, we refer to this as the ‘‘Eocene Phase’’. In front of the

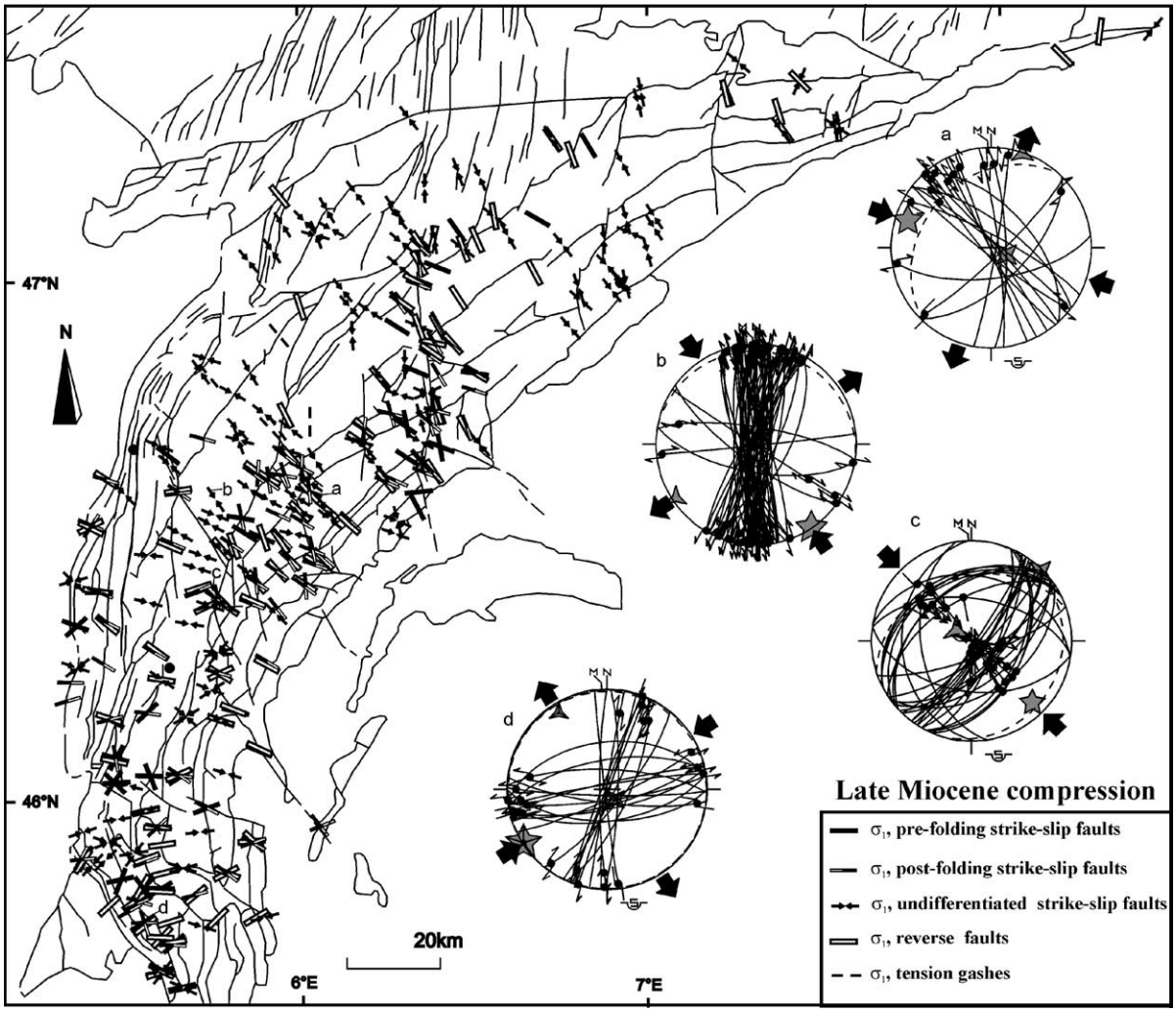

Fig. 7. The Late Miocene stress fields. Examples of fault-slip data are shown for four sites. Same symbols as in Fig. 1.

northern Jura frontal thrust, few small-scale folds are sealed by Middle to Late Oligocene strata (see Bergerat and Geyssant, 1987 for a review). In the Rhine Graben, about 40 km north of the Jura frontal thrust, minor fault-slips defining a N–S strike-slip compression affect Oligocene strata and predate brittle features related to the Oligocene E–W extension (Larroque, 1987). In the central Jura, a local unconformity with the Late Oligocene to Middle Miocene strata lying on Cretaceous or Jurassic strata (Aubert, 1958) may be interpreted as indicators of moderate flexures due to compressional Eocene–Oligocene tectonics. An alternative is that this unconformity (as that recognized to the NE between Early Miocene and Middle Miocene) reflects flexures related the Alpine foreland bulge (Laubscher, 1992).

Faults and fractures indicating a similar N–S strike-slip compression have been related by some authors to the west-European Oligocene rifting (Illies, 1975; Buchner, 1981). The N–S strike-slip tectonics in the Jura Mountains is very unlikely the product of the Rhine–Bresse rifting for two reasons. Firstly, brittle structures associated with the Eocene N–S compression clearly predate the Oligocene normal faulting. Secondly, the Eocene and Oligocene stress trajectories in the Jura Mountains differ radically (compare Figs. 4 and 5), indicating that the driving mechanisms of the Jura deformation during Eocene and Oligocene were not the same. The most likely sources of forces during Eocene are the Pyrenean collision (“Pyrenean orogeny”) some 400 km south of the Jura Mountains. Elsewhere in the southern France (Provence and Languedoc), intra-plate deformation from Campanian to Early Oligocene, mostly consisting of E–W thrusts and folds, has been related the Pyrenean orogeny (e.g., Bergerat, 1987; Tempier, 1987; Lacombe et al., 1992; Arthaud and Laurent, 1995; Rocher et al., 2000). We believe that the minor faulting associated with the N–S compression also corresponds to the expression of the Pyrenean orogeny in the Jura Mountains.

The N–S compression has been recognized in a large number of sites in the central Jura. No clear concentrations of features related to the N–S compression have been recognized, making it difficult to identify large faults associated with the Eocene Phase. However, it is striking that, while in the internal part of the belt the number of dextral and sinistral minor faults is equivalent (see site b in Fig. 4), the sinistral NE–SW minor faults largely dominate in the external Jura (Fig. 1A and site c in Fig. 4) and occur near major faults that have a NE–SW orientation. Such relations between minor and major faults are not fortuitous. As no abrupt lithological contrast in the cover has been reported, such weakness zones correspond to mechanical discontinuities in the underlying rocks, usually faults. During Eocene time, NE–SW sinistral faults have thus probably developed in the cover of the external Jura (Fig. 4), especially near the present “Euthe Pinçée”, “Pupillin Pinçée” and “Mamirolle Pinçée” (5, 4, 2 in Fig. 3).

Surprising is that the N–S compression is so poorly recognized in the Jura limbs (Fig. 4). Although the eastern part of the Jura was little investigated by the authors, the absence of the N–S compression may be related to the difficulty in recognizing it. Indeed, the Late Miocene compression may adopt a similar direction in this area (see Fig. 7). Pre-folding features defining a N–S compression may either correspond to the Eocene Phase or to the first Late Miocene deformation. Such an ambiguity may be solved by careful examination of the chronological relationships between the strike-slip faults and the normal faults related to the Oligocene tectonics. E–W local reverse faulting and moderate folding may have occurred in the eastern Jura during the Eocene as suggested by flexures sealed by Oligocene strata and minor reverse faults (Fig. 4). It is more enigmatic that the Eocene Phase was rarely recognized in the southern Jura. It may be related to the superposition of a NE–SW compression during the Late Miocene tectonics (see next section and Fig. 7).

4.2. The Oligocene extension

An E–W to NW–SE extension was recognized in 35 sites (Fig. 5). It is documented by steeply dipping N10°E to N50°E normal faults (sites a and c in Fig. 5). Numerous sub-vertical tension gashes averaging NNE–SSW in trend have also been found in the external central Jura (site b in Fig. 5) and are in agreement with such an extension. Most of the normal faults are encountered in the flat-lying beds of the external Jura. Near the western thrust front and in the internal part of the belt, the normal faults clearly predate folding. In seven sites, relative chronology

between brittle structures confirms that the normal faulting predates Late Miocene tectonics. Relative chronology criteria include reactivation of the extensional brittle structures during the Late Miocene compression, like sinistral slips on the NNE–SSW tension gashes and dextral slips on the NE–SW normal fault planes (Fig. 1).

Thus, the WNW–ESE extension predates the Late Miocene fold-and-thrust tectonics. It postdates Lower Cretaceous because it affects Valanginian formations. It follows the N–S compression (Fig. 1 and see previous sub-section). During the Oligocene, the west-European platform was affected by a rifting episode that produced the Bresse and Rhine Grabens. Early vertical movements occurred in Late Eocene in the Rhine Graben and intense faulting and subsidence began in the Early Oligocene. By the Late Oligocene, the two basins were filled and tectonic activity decreased. Minor fault analysis indicates that the direction of extension trends almost E–W near the Rhine Graben and WNW–ESE near the Bresse Graben (Bergerat, 1987; Villemin, 1987; Larroque and Laurent, 1988). About 20 km to the north of the eastern Jura frontal thrust, fibrous tension gashes in the Sannoisian indicate that the extension trends E–W (Larroque and Ansart, 1984). Twenty kilometer southward, within the Jura belt, Lacombe and Angelier (1993) reported normal faults affecting Oligocene formations and defining a NW–SE extension. Although the direction of extension slightly differs in the Jura from that in the neighboring grabens, we believe that the E–W to NW–SE extension recognized in the Jura belt corresponds to the Oligocene rifting episode. The irregular stress trajectory suggests that other mechanisms influenced the Oligocene normal faulting in the Jura belt. They are discussed in the last section.

Good documentation in the central external Jura allows consideration of the spatial distribution of minor faults. Particularly striking is that along the "Euthe Pincée" and the southern extension of the "Syam Faisceau" (5 and 6 on Fig. 3), minor normal faults are abundant whereas they are absent in sites situated only a few kilometers away from these two fault zones. As discussed in the first section, such concentration of minor deformation is indicative of large-scale faulting. The so-called "pincées" of the Jura plateaus, like the "Euthe Pincée", correspond to narrow collapsed zones bounded by two major faults and are classically interpreted as small grabens (Glangeaud, 1949; Mathis, 1974). Late Miocene deformation in these areas usually consists of intense folding and is restricted to the collapsed bands whereas the borders remained undeformed (see Fig. 10 for the horst case), indicating that the graben existed before the main fold-and-thrust tectonics. The concentration of minor deformation near the "Euthe pincée" thus demonstrates that minor fault analysis is relevant for the recognition of early large-scale faulting. In one site located along the "Euthe Pincée", normal slip data postdate the bed tilting (Fig. 1), suggesting that the Oligocene normal faulting has induced local, moderate tilting. Most minor faults along the southern extension of the "Syam Faisceau are west dipping. Assuming that minor faults mimic major ones, the normal fault-slip data along the southern extension of the "Syam Faisceau" correspond to large-scale west-dipping faults.

Similarly, the minor normal faults recognized along the "Pupillin Pinçée", the "Mamirolle Pinçée" (4 and 2 in Fig. 3) and other NNE–SSW faults (Fig. 5) very likely express major Oligocene normal faulting along these fault zones. However, it cannot be evidenced through analysis of minor fault frequency as the site distribution is not appropriate (some areas have not been investigated). Other faults in the Jura Mountains exhibit normal offsets of strata and will be described in the last section.

4.3. The minor NE–SW extension

Minor normal vectors defining an average NE–SW extension have been found in eight sites (Fig. 6). These normal faults trend N090°E to N170°E. The faulting–folding relation was recognized in the five sites; the NE–SW extension predates folding. The youngest strata affected by the NE–SW extension are Hauterivian. As most of these normal faults occur near the Morez and the Vuache tear Faults (7 and 9 in Fig. 3), this local extension could reflect the thrust-parallel stretching during the fold-and-thrust tectonics required by the divergence of the displacement vectors within the belt (Laubscher, 1972; Hindle and Burkhard, 1999). However, we find it unlikely as no normal slips coeval or postdating folding have been observed. Several tens of kilometers northwest of the

Jura (Lacombe, 1992) and east of the Rhine Graben (Bergerat and Geyssant, 1987), a pre-Eocene NNE–SSW extension has been identified and related to the latest Cretaceous rifting stage in northern Europe (see Dercourt et al., 2000 for a review). A similar direction of extension exists in the Paris basin, but has been assigned to the west-European Oligocene rifting (Coulon and Frizon De Lamotte, 1988). If the NE–SW extension is Oligocene in age, it would represent a surprisingly large counterclockwise stress rotation of about 70° relative to the other Oligocene extensional trends in the Jura, which are WNW–ESE on average.

A large part of the NW–SE minor normal faults has been found near the NW–SE Vuache and the Morez Faults (9 and 7 in Fig. 3). Unpublished seismic profiles studied by one of us (YP) suggest that during Oligocene, the Vuache Fault was a synsedimentary northeast-dipping normal fault. East of the Vuache Fault, Oligocene strata are two times thicker than west of it. The Morez Fault may also have undergone normal faulting, but these movements were moderate as no large offset in the Jurassic strata exists. Both the WNW–ESE and the NE–SW extensions may have produced the normal offset along the Vuache Fault. Whatever the age of this normal faulting, the Vuache Fault (and probably the Morez Fault) obviously already existed prior to the Late Miocene tectonics.

5. The Late Miocene stress fields

5.1. Minor fault attitude

In all but 14 of the investigated sites, the remaining fault-slip data (86% of the total population) result from stress states with horizontal σ_1 trending almost perpendicular to major thrust and fold axes (Fig. 7). Thus, they were assigned to the main Late Miocene fold-and-thrust tectonics. Three hundred twenty four stress tensors were calculated. Brittle structures are strike-slip and reverse faults, tension gashes and stylolitic peaks. Their orientations vary depending on whether they occurred in the central part of the Jura arc or at its limbs. In the eastern Jura, sinistral faults trend N160°E to N20°E and dextral ones N80°E to N130°E. In the central Jura, their respective orientations are N140°E to N10°E and N45°E to N120°E (sites a and b in Fig. 7). The trend of reverse faults varies from N030°E to N90°E in the eastern part of the belt, and from N–S to N90°E in the central part (site c in Fig. 7). With few exceptions, the Late Miocene minor fault population in the southern Jura (Fig. 7) defines two superposed compressions (Homberg et al., 1999, Fig. 2). The first fault subset consists of N080°E to N100°E sinistral faults, N–S to N040°E dextral ones, and N110°E to N30°E reverse ones. N130°E to N–S sinistral slips, N70°E to N110°E dextral slips, and N170°E to N45°E reverse ones define the second subset. Near the southernmost frontal thrust (the so-called "Bugey Faisceau", 11 in Fig. 3), N60°E to N100°E sinistral faults, N145°E to N20°E dextral ones (site d in Fig. 7), and N105°E to N65°E reverse ones define the first subset. The second subset strikes N130°E to N–S, N040°E to N135°E, and N140°E to N30°E. This change in minor fault attitude within the Jura belt results from a fan-shaped distribution of σ_1 trajectories (Fig. 7), in agreement with the arcuate shape of the major structures (see below for the discussion of stress trajectories).

Minor slip occurred both on newly formed and inherited planes. In the central and eastern Jura, inherited planes correspond to the N–S to NE–SW tension gashes and faults formed during the Eocene and Oligocene tectonics, and NW–SE faults formed during the Eocene tectonics. During the Jura Phase, sinistral slip occurred on the N–S to NNE–SSW and NW–SE planes, whereas dextral slip occurred on the NE–SW planes (Fig. 1). Some moderately dipping N–S to NE–SW planes (moderate dip being primary or acquired after bed tilting) were also reactivated as reverse faults. In the southern Jura, brittle structures that developed during the first Late Miocene compressional stage were reactivated during the second one. Hence, WNW–ESE planes underwent both an early sinistral slip and a late dextral one. Similarly, NW–SE to NNW–SSE gently dipping faults have undergone several event of reverse slip.

5.2. Stress regimes

Strike-slip faults were found in 172 sites (Fig. 7). In 21 sites, the strike-slip fault population has both pre-folding and post-folding slip vectors. In 24 sites, exclusively pre-folding slip vectors are present,

whereas in 53 sites only post-folding slip vectors were found. There is no ambiguity concerning the tectonic origin of the pre-folding faults. In all, but 12 sites, they define a similar stress state as the post-folding strike-slip faults. Moreover, in most sites, the compression that produced early slip is perpendicular to the major thrusts and fold axes. These pre-folding faults thus correspond to early deformation associated with Late Miocene tectonics. Except for two sites, no pre-folding reverse vectors were found. Because the pre-folding vectors consist exclusively of strike slips, the Jura Phase very likely started with a strike-slip regime.

The post-folding stress regime varies within the belt (Fig. 7). In the flat-lying and weakly deformed parts of the external Jura (“Jura des Plateaux”), all Late Miocene minor faults are strike-slip faults (see site b in Fig. 7). Although the gentle bed tilt prevents the establishment of the chronology between faulting and folding, we believe that the strike-slip regime probably persisted during the whole Jura Phase in these areas. An alternative is that the stress regime in the “Jura des Plateaux” switched during the Jura Phase from an early strike-slip regime to a late reverse one. The absence of reverse faults would then be explained by low shear stresses. However, we find this unlikely because it implies that shear stresses were first high, inducing strike-slip faults before folding, and then decrease during the folding and thrusting tectonics. Outwards the “Jura des Plateaux”, reverse faults were found in 78 sites. In highly folded areas, with two exceptions, reverse faults systematically postdate folding. Considering that folds in the southern and central Jura are transported detachment folds or fault-propagation folds (Martin and Mercier, 1994, 1996; Philippe et al., 1996), the scarcity of syn-folding reverse faults suggests that minor faulting did not develop in the uppermost cover rocks until the thrust ramp had reached the surface. However, reverse minor slips in the uppermost cover coeval to folding should not be excluded. Indeed, some bedding planes carry reverse striae (see site c in Fig. 7). Such slip vectors may have occurred at an intermediate stage of bed tilting. The reverse regime has thus probably prevailed in the internal Jura since folding began.

In the internal part of the belt and near major thrusts of the external Jura, the early strike-slip regime was thus followed by a reverse one. However, among the 83 sites showing minor slip vectors that clearly postdate folding, post-folding fault population consists either exclusively of strike slips at 23 sites, exclusively of reverse slips at 9 sites, or both strike slips and reverse slips at 51 sites. Among the post-folding data, some reverse faults postdate strike slip ones. In most sites where post-folding strike-slip and reverse faults co-exist, they define the same direction of compression. The two stress regimes are thus related through σ_2/σ_3 stress permutation. Such σ_2/σ_3 stress permutation is explained by Laubscher (1972) by a decrease in the horizontal stress perpendicular to displacement (that is approximately parallel to fold axis) due to necessary stretching related to the divergence of displacement trajectories within the arcuate belt. Stretching is accommodated by tear faults where the horizontal stress parallel to fold axes has been converted from σ_2 (reverse regime) to σ_3 (strike-slip regime). Indeed, 43 of the sites showing post-folding strike-slip faults are located close (less than 2.5 km) to major tear faults (Fig. 7), such as the Pontarlier Fault, the Morez Fault and the Vuache Fault (3, 7 and 9 in Fig. 3). In few sites, the attitude of the strike-slip vectors changes progressively from pre-folding to post-folding slip vectors (see site a in Fig. 7), confirming that folds have developed there in a strike-slip regime. Near such faults, although the stress regime was dominantly of strike-slip type, few minor reverse faults have also developed due to the proximity of active thrusts. Away from the large-scale strike-slip faults, late minor strike slips are more surprising. They occurred in 31 sites. It may indicate that small, undiscovered tear faults exist, as suggested by Hindle and Burkhard (1999).

5.3. Stress deflections indicate crustal heterogeneities

Within structural domains, stress orientations are generally homogenous at large-scale and reflect regional boundary conditions, i.e., plate movement (e.g., Angelier, 1979; Mercier et al., 1979; Bergerat, 1987; Le Pichon et al., 1988; Zoback et al., 1989). However, local stress deflections exist. The stress state may change because the crust is a rheologically discontinuous medium, exhibiting weakness planes (e.g., faults), topographic reliefs, and weak “inlusions” (e.g., basins) contrasting with strong ones (e.g., basement highs). Stress deflections can be

viewed as indicators of crustal heterogeneities and their dynamics. Such an approach has been used to characterize the kinematics of indenters (Homberg et al., 1999) and to recognize successive slip events on major faults (Homberg, 2000).

At the first order, the directions of compression of the Jura Phase are arranged in a fan-shaped pattern around a NW–SE direction (Fig. 7). This stress distribution has been recognized early by the pioneer Jura workers (e.g., Laubscher, 1972; Plessmann, 1972). Other workers (Fig. 3 and Sopena and Soulas, 1973) have refined the stress trajectories (Fig. 7). Pre-Neogene palinspastic reconstructions show that the fan-shaped pattern cannot be the product of gravity sliding (Laubscher, 1973). It rather indicates that the Jura was indented by its stronger hinterland (Laubscher, 1972; Vialon et al., 1984; Burkhard, 1990; Hindle and Burkhard, 1999; Homberg et al., 1999). The regular NE–SW strikes of thrusts and folds in the external Alps behind the Jura suggest that the Adriatic lithospheric indenter did not produce significant stress deviation in the Jura Mountains. Stress directions were probably uniform in the basement judging from the present-day regular NW–SE trend of *P*-axes in focal mechanisms below the basal décollement level (Pavoni, 1980; Deichmann, 1992). The fan-shaped pattern in the cover during the Jura Phase must thus be related to a shallow indenter, either the thrust pile of the external Alps or the thick Molasse Basin where the thickness of the cover exceeds by several kilometers that of the Jura Mountains. The internal Jura may have also behaved as a deformable indenter compared with the external part of the belt, due to the greater thickness of its cover relative to that of the external Jura (Philippe et al., 1994). Whatever the nature of the indenter, its dynamics induced a change of the stress trajectory during the Jura tectonics. Indeed, while in the eastern and central Jura, the pre-folding and post-folding directions of compression are similar, two different compressions, WSW–ESE and WNW–ESE on average, have been recognized in the southern Jura (Fig. 7). In this area and from north to south, the first compression trends N60°E to N45°E. It is documented by pre-folding strike-slip faults (site d in Fig. 7). The second one trends N120°E in the north to N90°E in the south and consists of post-folding slip events, both strike slip and reverse. Considering the whole Jura belt, the pre-folding and post-folding stress trajectories differ; both are fan-shaped, but the deviation of the compression is much higher in the southern Jura for the early stress field (Fig. 7). Because the early stress field is also documented by some post-folding minor strike-slip and reverse faults, we can assume that it persisted after folding. It thus governed most of the large-scale deformation in the Jura Mountains. The second one corresponds to the very late Jura tectonics (see Fig. 8).

Whatever the accurate age of the successive stress fields, the stress trajectory changed during the Jura tectonics in the southern part of the belt. Lateral impersistence of the Triassic evaporites and salt layers (the basal décollement of the Jura cover) towards the Ile Cremieu (Philippe et al., 1994) may have given rise to stress deviations in the southern Jura. However, it does not account for the radical change in the stress trajectory during the Jura Phase. Homberg et al. (1999) have suggested that the large stress rotation in the southern Jura during the first Late Miocene compressional stage corresponds to a major decoupling within the Molasse Basin along the Vuache Fault (9 in Fig. 3 and see Fig. 8C, D). The Molasse Basin later behaved as a single block, stress distribution in the Jura corresponding then to a symmetric fan with moderate angle. Based on map restorations and field data, Philippe et al. (1994) suggested that deformation in the southern Jura is partitioned along a set of tear faults (the so-called "Pont d'Ain-Culoz" fault zone, 10 in Fig. 3) into pure shear strain in the most external and internal Jura, and simple-shear strain along the external–internal boundary. Both mechanisms proposed by Philippe et al. (1994) and Homberg et al. (1999) agree with a decoupling along NW–SE to WNW–EWE faults, but differ on where this decoupling occurred.

Besides the general fan-shaped stress distribution, second order (i.e., at small-scale) stress deviations have been identified. Most of them occur near major faults, like the Morez Fault and the Pontarlier Fault (3 and 7 in Fig. 3). Near the Morez Fault, the compression rotates counterclockwise by about 20°, so that it tends to become perpendicular to the fault strike (Fig. 7 and see Fig. 2 in Homberg et al., 1997). Numerical modeling has shown that these stress deflections attest to the presence of a thin weak NW–SE zone along the Morez Fault (Homberg et al., 1997). Such a local

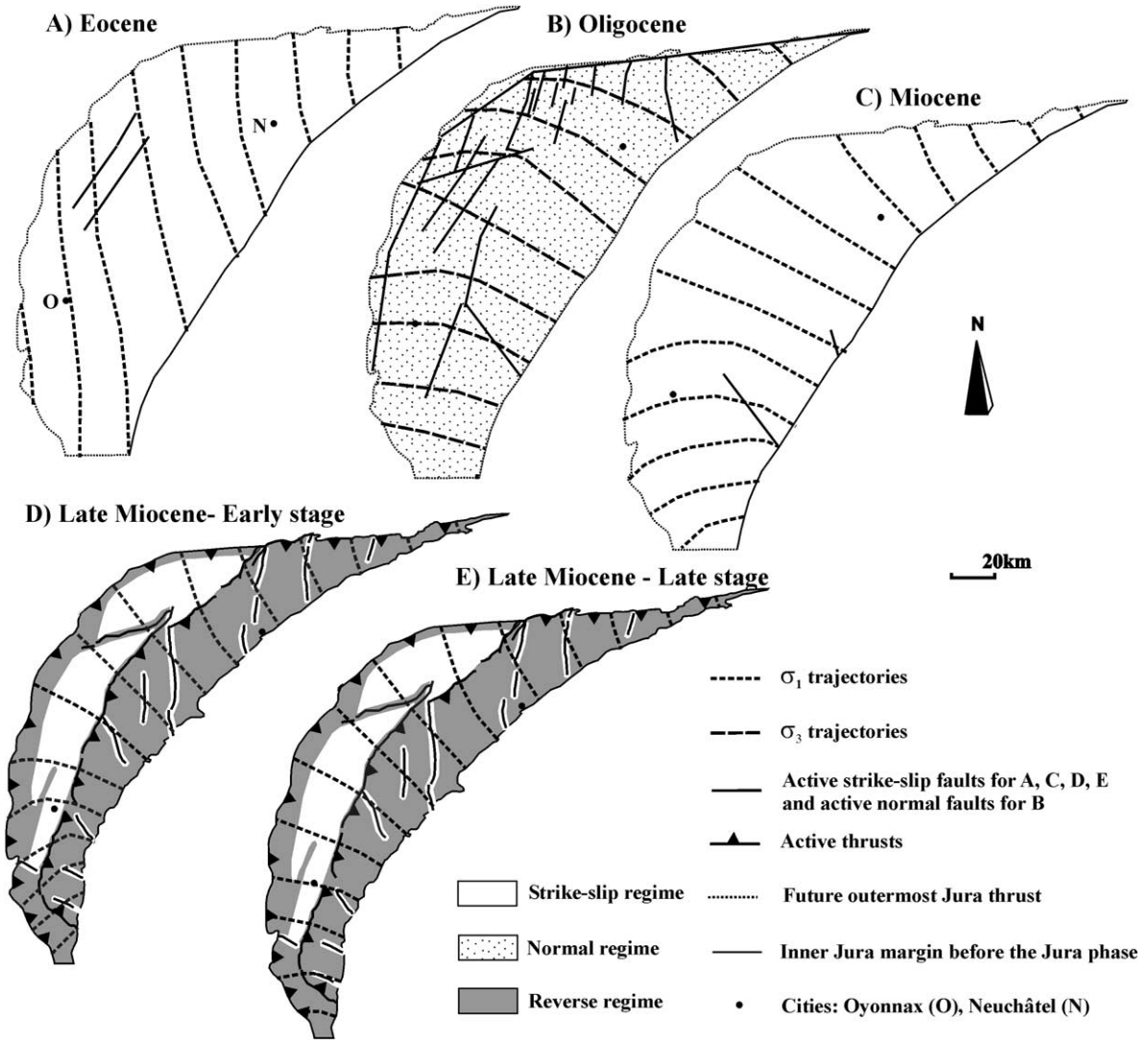

Fig. 8. Cenozoic evolutionary model of the Jura. Stress fields and faulting during the major Cenozoic tectonic events are shown. For stages (A), (B), and (C), stresses, faults, and Jura margin are considered with their palinspastic positions using the map restoration of Philippe et al. (1996). For clarity, local stress orientations are not shown (see Figs. 4–7). For stages (D) and (E), only major faults are figured.

weakness within the crust suggests early tectonics, which may have occurred either during the N–S Eocene compression (Fig. 4) or the NE–SW extension (Fig. 6), as revealed by NW–SE dextral and normal minor faults along the Morez Fault. Near the Pontarlier Fault, the Late Miocene stress field is largely heterogeneous, exhibiting both clockwise and counterclockwise rotations of compression near the fault (Fig. 7). Locally, two superimposed compressions exist. Numerical models of the stress field following a rupture have demonstrated that the complexity of the stress field in this area corresponds to the stress signature of two successive rupture events along the Pontarlier Fault (Homberg, 2000). The first one occurred before folding and implies the southern segment of the Pontarlier Fault (Fig. 8C). The second event is a rupture of the whole Pontarlier Fault and occurred later in the Jura Phase.

6. Tertiary evolutionary model of the Jura Belt

Using the map restoration of Philippe et al. (1996) which is based on serial balanced cross-sections, we present a structural evolutionary model of the Jura fold-and-thrust belt during the Cenozoic (Fig. 8). Because its tectonic history is poorly documented and apparently did not give rise to major structures, the Mesozoic is not considered herein. Five palinspastic maps showing the stress field and major active faults at different key periods are presented. The two first maps concern the pre-orogenic Jura deformations in Eocene and Oligocene times (Fig. 8A and B). The third one (Fig. 8C) illustrates the first stage that followed the drastic change in the Jura tectonic context from Oligocene rifting to Alpine orogeny. It probably started just prior to the Late Miocene. The fourth and fifth maps (Fig. 8D and E) show the two steps of the Jura fold-and-thrust tectonics that occurred at Late Miocene time. The stress trajectories have been manually drawn, using local stress orientations inferred from minor fault inversion (Figs. 4–7). For the first three maps, the stress trajectories are derived from the local stress states corrected for displacements and rotations after restoration of the cover. Active faults during the pre-orogenic phases are deduced from the minor fault analysis presented above, as well as from the previous works. They are shown in their palinspastic positions. For simplicity, the normal faulting on the Morez Fault and the Vuache Fault (Fig. 6) are shown in the Oligocene map. As discussed before, even if inherited from earlier tectonics, these faults were obviously reactivated during the Oligocene extension.

6.1. Cover and basement deformation during the Paleogene

In the Eocene, the Jura was a platform, with an about 2 kilometers thick sedimentary pile. Stress state was a strike-slip regime, with the maximum stress axis trending NNW–SSE to N–S (Fig. 8A). Shear stresses were probably low, so that the Jura platform was a relatively stable domain. However, in a few areas, fault-slip analysis indicates that the differential stress level was large enough to induce moderate faulting (Fig. 8A). In the central Jura, faulting consists of a few sinistral sub-vertical strike-slip faults along the future "Pupillin Pinçée" and "Euthe Pinçée". Reverse faulting and folding may have occurred in the eastern Jura, near the future frontal thrust.

During the Oligocene, the stress regime in the Jura platform radically changed, switching to an extensional regime (Fig. 8B). At that time, the Jura was a transitional domain between the ongoing rifting-related Bresse and Rhine Grabens (as well as the connecting Rhine–Saône transform fault) and the foredeep Molassic Basin controlled by the load of the Alps thrust pile (Sissingh, 1998). These complex boundary conditions induced a heterogeneous stress field in the Jura belt (Fig. 8B). In the central Jura, the direction of the extension progressively changed from E–W near the western margin of the Jura to NW–SE in the internal part. In the Jura limbs, the extension is poorly documented, but may show similar deviations. Such stress deflections reflect that faulting in the Jura platform during Oligocene was genetically related to both the Molasse Basin and west-European rift development. In the central and northeastern external Jura, the Rhine–Saône transform motion and the inherited NE–SW Eocene zones of weakness within the cover also induced local stress deviations (Lacombe et al., 1993; Homberg et al., 1994).

N–S to NE–SW rifting-related normal faulting occurred in the external Jura (Fig. 8B). In the westernmost central Jura, NNE–SSW normal faults, striking parallel to the eastern margin of the Bresse Graben, offset the Jura Mesozoic strata. Although some of them may be the result of late local gravity sliding after the Jura Phase (Mugnier and Vialon, 1986), most of these faults probably formed during the Oligocene rifting episode (Chauve et al., 1988), as suggested by the minor pre-folding normal slips (Fig. 5). At that time, this part of the Jura was situated about 10 km eastward of the "Grande Faille Bordière", the major normal basement fault zone bordering the Bresse Graben to the east. Well data clearly show that normal faults affect the basement between the "Grande Faille Bordière" and the western margin of the Jura platform. As proposed in the balanced cross-section by Chauve et al. (1988), the normal faults identified in the cover of the western central Jura probably extend into the basement. Oligocene normal faulting in the Jura Mountains is not confined to the proximity of the Bresse Graben. In the central external Jura, the rifting tectonics is responsible for

NNE–SSW to NE–SW normal faults with offsets of several hundreds of meters. Some of them defined narrow grabens, a few hundreds of meters large, such as along the future "Euthe Pinçée", "Pupillin Pinçée", and "Mamirolle Pinçée" (Figs. 8B and 9B). Like the minor normal slip vectors (Fig. 5), these faults are steeply dipping. There is probably a causal relationship between this high inclination and the cover

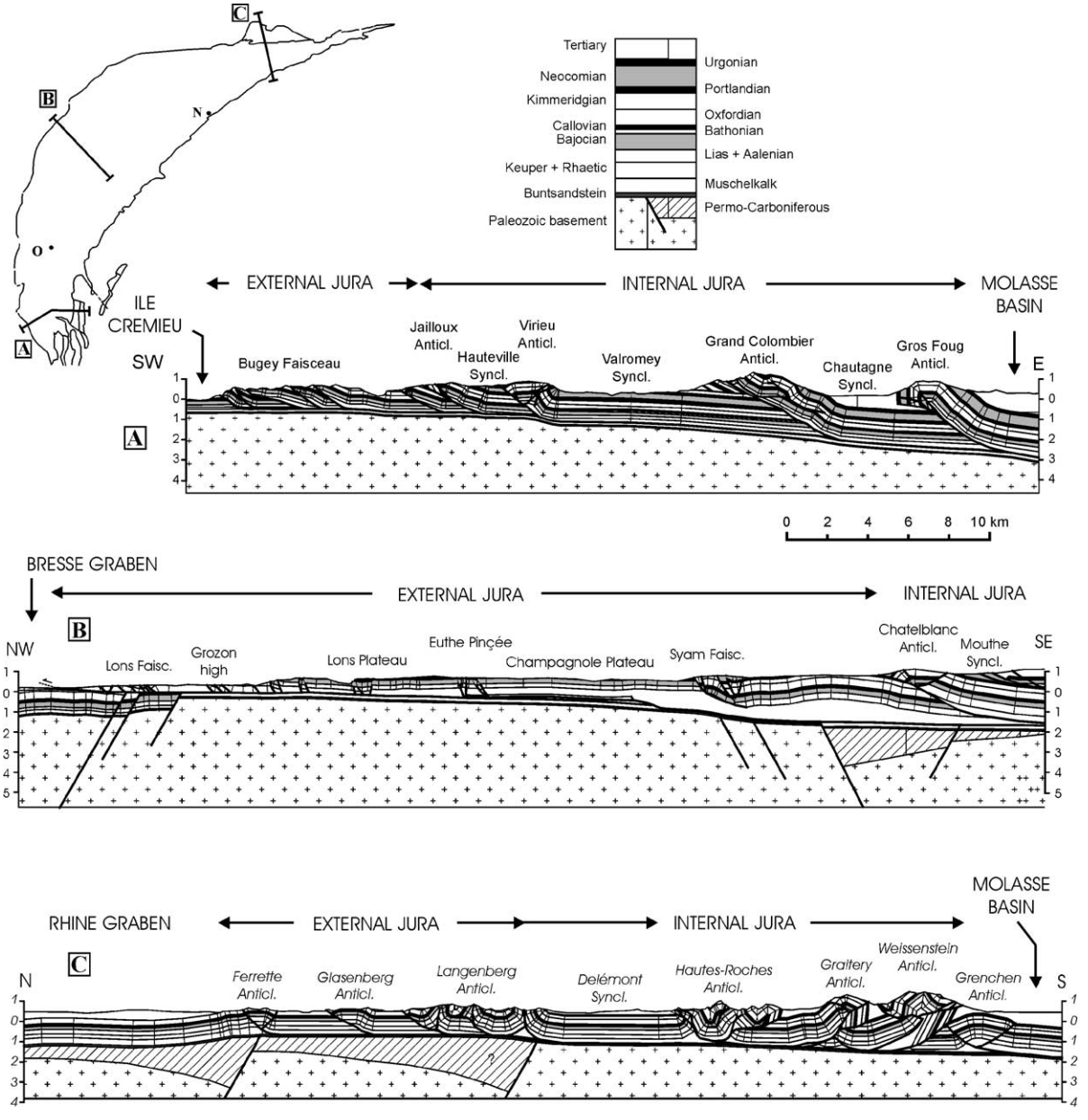

Fig. 9. Structural characteristics of the external Jura. Balanced cross-sections from Philippe et al. (1996). Cities: Oyonnax (O) and Neuchâtel (N). Pre-orogenic faults and pinch outs of the décollement levels to the south have controlled the amount of displacement along the front thrust of the Jura onto the foreland and the structural characteristics of the external Jura. See explanations in the text.

discontinuities inherited from the Eocene tectonics (Fig. 8A). To the east, in the present Syam Faisceau (Fig. 9B), vertical offset has been related to an east-dipping NNE–SSE normal fault (Mugnier and Vialon, 1986; Guellec et al., 1990; Philippe et al., 1996). In the southern extension of the Syam Faisceau, minor fault analysis suggests that west-dipping normal faulting occurred along the present-day Jura external–internal boundary (Fig. 5). Assuming that the regular trend of this structural boundary is not fortuitous, the present western boundary of the internal Jura was an active deformation zone during the Oligocene extensional tectonics (Fig. 8B). In the northern central Jura and in the eastern Jura, vertical offsets of several hundreds of meters on the flat-lying beds along NNE–SSW faults are very likely related to the Oligocene rifting (Fig. 8B).

In the eastern Jura, beside rift-related N–S normal faulting, Oligocene deformation, probably genetically related to the Molasse Basin and/or the transform fault connecting the Bresse and Rhine Grabens, occurred near the present Jura frontal thrust. They are referred to as faulted flexures (Laubscher, 1986) and result from the deep reactivation of average WNW–ESE striking faults bordering the underlying Paleozoic trough which induced offsets or flexures of the Triassic décollement levels. These deep normal faults are thought to extent westward along the Jura northern front. Below the "Bisontin Faisceau" (1 in Fig. 3), north-dipping basement faults have been recognized. Martin and Mercier (1996) suggest that the ENE–SSW normal faults in the overlying cover extent into the basement. In these areas, normal faulting was probably controlled by the transtensional motion along the Rhine–Saône transform zone (Lacombe et al., 1993). In the internal Jura, Oligocene normal faulting occurred on a few NW–SE northeast-dipping faults like the Vuache Fault (and maybe the Morez Fault).

The relationships between the Oligocene cover and basement deformation are not clear. Near the external border of the Jura, normal faults recognized in the cover are thought to extend into the basement (Chauve et al., 1988; Martin and Mercier, 1996). This is also probably the case for the normal faults along the present external–internal Jura boundary. Indeed, the abrupt increase in depth of the Paleozoic layers near the external–internal Jura boundary could correspond to vertical offset along two east-dipping normal faults (Philippe et al., 1996). The easternmost one coincides with the palinspastic emplacement of the east-dipping fault recognized in the cover along the Syam Faisceau. Concerning other normal faults in the interiors of the Jura, like those along the future "Euthe Pinçée", "Pupillin Pinçée", and "Mamirolle Pinçée, no relation between their palinspastic positions and discontinuities in the basement has been recognized. Unpublished seismic profiles studied by one of us (YP) show deep faults with vertical offsets in the basement that end in the Trias décollement levels. This may suggest that the thick Trias plastic levels have prevented propagation into the cover of the deep normal faulting during the Oligocene. Whether or not Oligocene deformation in the Jura cover was decoupled from that of the basement is an open question.

6.2. Late Miocene fold-and-thrust tectonics and the role of structural inheritance

In Miocene time, the Jura consisted of an heterogenous sedimentary wedge. Heterogeneities were (1) weakness zones in the cover and offsets (or flexures) of the gently SE-dipping décollement levels inherited from pre-orogenic tectonics (Fig. 8A and B), (2) thickness variations of the Triassic décollement levels, and particularly pinch outs in the southern Jura, and (3) progressive taper of the wedge toward the foreland, related to the paleogeography during Meso-Cenozoic deposits and the erosion during Oligocene along the western edge of the Jura.

After the Oligocene, the Alpine push brought the Jura domain into a compressional context. An initial strike-slip regime prevailed in the whole belt (Fig. 8C), with a fan-shaped distribution of the compression directions, due to the Jura indentation by its hinterland. At that time, the stress level was too low to create major deformation. Moderate deformation may have locally occurred, like the early sinistral slip evidenced on the southernmost segment of the Pontarlier Fault (Homberg, 2000). The strong deviation of the stress trajectory in the southern Jura also suggests a major decoupling along the pre-existing Vuache Fault (Homberg et al., 1999). Later on, the increasing Alpine push induced a reverse regime in the internal Jura (Fig. 8D). As it was undercritical, the internal

Jura underwent internal strain, resulting in large overthrusts and associated fault-propagation folds in the central and southern part of the belt (Fig. 9A, B), as well as detachment box folds in the eastern Jura (Fig. 9C). The divergence of the displacement vectors led to the development of tear faults in the cover (Fig. 8D). Near these faults, the stress regime switched from reverse to strike slip through σ_2/σ_3 stress permutation. Weakness zones in the cover inherited from previous tectonics (Fig. 8A and B) strongly influenced the location of these tear faults, like the Vuache and the Morez Faults. They induced mechanical decoupling within the cover, the blocks on either sides of these transfer faults deforming independently. In the central Jura, thrusts initiated close to the pre-existing Oligocene normal faults to form the present external–internal Jura boundary. It is striking that the dip directions of thrusts are identical to those of normal faults; in the Syam Faisceau (which strictly speaking does not belong to the internal Jura), the Oligocene normal faults dip to the east (Fig. 9B) and the thrust vergence is to the west. To the south, the Oligocene normal faults dip to the west and the Late Miocene deformation is taken up by one major backthrust (the east-vergent Oyonnax Thrust, 8 in Fig. 3).

Faulting and folding of the internal Jura prevented the full stress transmission to the NW, so that the stress regime remained of strike-slip type in the external Jura where no large deformation occurred (Fig. 8D). However, stress concentrations and stress permutations occurred near pre-existing fault-related offsets, flexures and pinch outs of the décollement levels (Laubscher, 1986; Philippe et al., 1996), as well as near the inherited cover discontinuities where thrusts nucleated and folding concentrated. The structural style of the external Jura varies according to the initial conditions (Fig. 9). In the eastern Jura limbs, ramps of the frontal thrust initiate at about 1-km depth, near the flexures and offsets of the décollement layers; the Jura cover thrusted about 2 km onto the foreland (Fig. 9C). In the central Jura, because of the intense Oligocene faulting and erosion near the eastern border of the Bresse Graben, epygliptic thrusting developed, authorizing a much larger horizontal displacement of about 10 km of the Jura cover (e.g., Chauve et al., 1988; Philippe et al., 1996) onto the Bresse Graben (Fig. 9B) whereas the external part of the belt underwent little deformation. In the southern Jura limbs (Fig. 9A), large thrusting and folding of the external Jura cover are related to the reduction of the décollement level thickness, until it pinches out near the Ile Crémieu, where the prism is characterized by high basal friction properties. In accordance with the critical taper model, closely spaced thrusts developed

Fig. 10. Example of Late Miocene deformation near the Oligocene faults. Outcrop of Callovian strata 1 km to the west of the Mamirolle "Pinçée" (2 in Fig. 3). Late Miocene deformation is restricted to the interiors of the Oligocene horst. The borders remained undeformed.

in the cover, resulting in a structural style strongly contrasting with that of the external central and eastern Jura (compare Fig. 8A, B and C).

Besides initiation of the frontal thrust, local thrusting and folding occurred in the external Jura near the pre-orogenic faults, like the already discussed Syam Faisceau (Fig. 9B). Moderate deformation occurred near the N–S to NE–SW weakness zones of the cover. A common deformation scheme consists in tight folding within narrow stripes bounded by the pre-existing faults, whereas the neighboring areas remained unaffected. The most spectacular examples are the so-called "Pinçées" (Fig. 9B), but similar local deformation occurred within the Oligocene horsts (Fig. 10). Strike-slip movements, like the dextral slip on the northern "Euthe Pinçée", or dip-slip movements, like the reverse motion along the southern "Euthe Pincée", occurred on Oligocene faults. Distribution of the Late Miocene deformation in the external Jura thus mimics the pre-orogenic structural pattern.

Later in the Jura tectonics, the stress field changed in the southern Jura (Fig. 8E). This change is probably related to an increase in coupling within the Molasse Basin cover along the Vuache Fault (Homberg et al., 1999). As was the case during the first deformation of the Jura Phase (Fig. 8D), both strike-slip and reverse regimes coexisted (Fig. 7). In the central and eastern Jura, stress regimes during the late stress field cannot be defined with certitude, as stresses remained coaxial during the whole Jura Phase (Fig. 7). It is likely that the pattern of reverse regime domains and strike-slip regime domains did not dramatically changed during the late compression, although the numerous minor strike-slip minor faults in the southern Jura may indicate that the strike-slip regime has affected larger areas. This late strike-slip stress field may reflect the decreasing Alpine push.

7. Conclusion

Analysis of minor fault-slip data has allowed characterization of the successive stress fields and active faults in the Jura Mountains during the Cenozoic. Two pre-orogenic events, a N–S Eocene strike-slip event and an Oligocene WNW–ESE extensional event, predated the main Late Miocene fold-and-thrust tectonics and produced N–S to NE–SW, NW–SE, and WNW–ESE faults. Comparisons between the Late Miocene stress fields and the pattern of pre-orogenic faults reveal that the inherited discontinuities have modified the Late Miocene stresses and were crucial for the structural development of the belt. Major fault zones, like those separating the flat-lying beds in the Plateaus of the external Jura, the western thrust of the central internal Jura, and the frontal Jura thrust onto the foreland, developed near the inherited discontinuities where stress concentration and/or permutation occurred. Other pre-orogenic discontinuities, like those near the Morez and Vuache tear Faults, induced major decoupling within the cover, isolating blocks that have deformed independently. Mechanical analysis of the Late Miocene stress deflections provided further evidences that some faults were inherited. This study shows that where macro-structural analysis is insufficient to recognize pre-orogenic tectonics in deformed belts, minor fault-slip analysis has the potential to define the pre-orogenic faults pattern and to highlight how inherited faults influence the development of fold-and-thrust belts.

Acknowledgements

We are grateful for the thoughtful reviews by Martin Burkhard and Ulrike Kastrup which allowed us to improve the manuscript. We thank Eric Barrier and James Grannath for the useful remarks. This work was supported by the Université Pierre et Marie Curie and the CNRS.

References

Anderson, E.M., 1942. The dynamics of faulting. Oliver and Boyd, Edinburgh, 206 pp.

Angelier, J., 1979. Néotectonique de l'arc égéen. Soc. Géol. Nord., Spéc. Publ. 3, Lille, 418 pp.

Angelier, J., 1984. Tectonic analysis of fault slip data sets. J. Geophys. Res. 89, 5835–5848.

Angelier, J., 1990. Inversion of field data in fault tectonics to obtain the regional stress: III. A new rapid direct inversion method by analytical means. Geophys. J. Int. 103, 363–376.

Angelier, J., Manoussis, S., 1980. Classification automatique et distinction des phases superposées en tectonique de failles. C. R. Acad. Sci. Paris 290, 654–661.

Angelier, J., Tarantola, A., Valette, B., Manoussis, S., 1982. Inver-

sion of field data in fault tectonics to obtain the regional stress: I. Single phase fault populations: a new method of computing the stress tensor. Geophys. J. R. Astron. Soc. 69, 607–621.

Arthaud, F., Laurent, P., 1995. Contraintes, déformation et déplacement dans l'avant-pays Nord-pyrénéen du Langedoc méditerranéen. Geodyn. Acta 8, 142–157.

Aubert, D., 1958. Sur l'existence d'une ride de plissement oligocène dans le Jura vaudois. Bull. Soc. Neuchatel. Sci. Nat. 81, 47–53.

Ballard, J.-P., Brun, J.-P., Van den Driessche, J., Allemand, P., 1987. Propagation des chevauchements au dessus des zones de décollement: modèles expérimentaux. C. R. Acad. Sci. Paris 305, 1249–1253.

Bergerat, F., 1987. Stress fields in the European platform at the time of Africa–Eurasia collision. Tectonics 6, 99–132.

Bergerat, F., Angelier, A., 2000. The south Iceland seismic zone: tectonic and seismotectonic analyses revealing the evolution from rifting to transform motion. J. Geodyn. 29, 131–211.

Bergerat, F., Geyssant, J., 1987. Paléo-champs de contraintes tertiaires dans le domaine jurassien entre Ajoie et Jura souabe. Bull. Inf. Geol. Bassin Paris 24, 25–36.

Brudy, M., Zoback, M.D., Fuchs, K., Rumel, F., Baumgärtner, J., 1997. Estimation of the complete stress tensors to 8 km depth in the KTB scientific drill holes: implications for crustal strength. J. Geophys. Res. 102, 18453–18475.

Buchner, F., 1981. Rhinegraben: horizontal stylolites indicating stress regimes of earlier stages of rifting. Tectonophysics 73, 113–118.

Burkhard, M., 1990. Aspects of the large-scale Miocene deformation in the most external part of the Swiss Alps (Subalpine Molasse to Jura fold belt. Eclogae Geol. Helv. 83, 779–780.

Burkhard, M., Sommaruga, A., 1998. Evolution of the western Molasse basin: structural relations with the Alps and the Jura belt. In: Mascle, A., Puigdefabregas, C., Luterbacher, H.P., Fernadez, M. (Eds.), Cenozoic Foreland Basins of Western Europe. Geol. Soc. Spec. Pub., vol. 134, pp. 279–298.

Buxtorf, A., 1907. Geologische Beschreibung des Weissenstein-Tunnels und seiner Umgebung. Beitr. Geol. Kt. Schweiz, 21.

Chauve, P., Martin, J., Petijean, E., Sequeiros, F., 1988. Le chevauchement du Jura sur la Bresse: données nouvelles et réinterprétation des sondages. Bull. Soc. Geol. Fr. 8, 861–870.

Choi, P.Y., 1996. Reconstitution des paléocontraintes en tectonique cassante: méthodes et applications en domaines déformés (Corée, Jura). Unpublished PhD Thesis, Univ. P. & M. Curie, Paris, 257 pp.

Cornet, F.H., Burlet, D., 1992. Stress field determinations in France by hydraulic tests in boreholes. J. Geophys. Res. 97, 11829–11849.

Coulon, M., Frizon De Lamotte, D., 1988. Les extensions cénozoïques dans l'Est du bassin de Paris. C. R. Acad. Sci. Paris 307, 1111–1119.

Davis, D., Engelder, T., 1985. The role of salt in fold-and-thrust belts. Tectonophysics 119, 67–89.

Davis, D., Suppe, J., Dahlen, F.A., 1983. Mechanics of fold-and-thrust belts and accretionary wedges. J. Geophys. Res. 88, 1153–1172.

Deichmann, N., 1992. Recent seismicity of the northern Alpine foreland. Eclogae Geol. Helv. 85, 701–705.

Dercourt, J., Getanai, M., Vrielynck, B., Barrier, E., Biju-Duval, B., Brunet, M.F., Cadet, J.-P., Crasquin, S., Sandulescu, M. (Eds.), 2000. Atlas Peri-Tethys, Paleogeographical Maps, CCGM/CGMW, Paris, 24 Maps and Explanatory Notes, vol. I–XX, 1–269.

Eldredge, S., Bachtadse, V., Van der Voo, R., 1985. Paleomagnetism and the orocline hypothesis. Tectonophysics 119, 153–179.

Gehring, A., Keller, P., Heller, F., 1991. Paleomagnetism and tectonics of the Jura arcuate mountain belt in France and Switzerland. Tectonophysics 186, 269–278.

Glangeaud, L., 1949. Les caractères structuraux du Jura. Bull. Soc. Geol. Fr. 5, 669–688.

Guellec, S., Mugnier, J.L., Tardy, M., Roure, F., 1990. Neogene evolution of the western Alpine foreland in the light of ECORS data and balanced cross-sections. In: Roure, F., Heitzmann, P., Polino, R. (Eds.), Deep Structure of the Alps. Mem. Soc. Geol. Fr., vol. 15, pp. 165–184.

Hauksson, E., 1994. State of stress from focal mechanisms before and after the Landers earthquake sequence. Bull. Seismol. Soc. Am. 84, 917–934.

Hindle, D., Burkhard, M., 1999. Strain, displacement and rotation associated with the formation of curvature in fold belt; the example of the Jura arc. J. Struct. Geol. 21, 1089–1101.

Homberg, C., 1997. Analyse des déformations cassantes dans le Jura et modélisation numérique des perturbations des contraintes tectoniques autour d'accidents majeurs. Unpublished PhD Thesis, Univ. P. & M. Curie, Paris, 306 pp.

Homberg, C., 2000. Ruptures and stress deflections. In: Bokelmann, G., Kovach, R.L. (Eds.), Proceedings of the 3rd Conference on Tectonic Problems of the San Andreas Fault System. Geo. Sci., Stanford Univ. Pub., Vol. XXI, Stanford, pp. 324–332.

Homberg, C., Angelier, A., Bergerat, F., Lacombe, O., 1994. Nouvelles données tectoniques dans le Jura externe: apport des paléocontraintes. C. R. Acad. Sci. Paris 318, 1371–1377.

Homberg, C., Hu, J.C., Angelier, J., Bergerat, F., Lacombe, O., 1997. Characterization of stress perturbations near major fault zones: Insights from 2-D distinct-element numerical modeling and field studies (Jura Mountains). J. Struct. Geol. 19, 703–718.

Homberg, C., Lacombe, O., Angelier, J., Bergerat, F., 1999. New constraints for indentation mechanisms in arcuate belts from the Jura Mountains, France. Geology 27, 827–830.

Huiqi, L., Mc Clay, K.R., Powell, D., 1992. Physical models of thrusts wedges. In: Mc Clay, K.R. (Ed.), Thrust Tectonics. Chapman & Hall, London, pp. 71–81.

Illies, H., 1975. Intraplate tectonics in stable Europe as related to plate tectonics in the Alpine system. Geol. Rundsch. 64, 677–699.

Jordan, P., 1992. Evidence for large-scale decoupling in the Triassic evaporites of Northern Switzerland: an overview. Eclogae Geol. Helv. 85, 677–693.

Kattenhorn, S.A., Aydin, A., Pollard, D.D., 2000. Joints at high angles to normal fault strike: an explanation using 3-D numerical models of fault-perturbed stress fields. J. Struct. Geol. 22, 1–23.

Lacombe, O., 1992. Maclage, fracturation et paléocontraintes intraplaques: application à la plate-forme carbonatée ouest-européenne. Unpublished PhD Thesis, Univ. P. & M. Curie, Paris, 316 pp.

Lacombe, O., Angelier, J., 1993. Evolution tectonique du Jura externe au Cénozoïque et perturbations de contraintes dans la zone transformante Rhin-Saône. C. R. Acad. Sci. Paris 317, 1113–1120.

Lacombe, O., Angelier, J., Laurent, P., 1992. Determining paleostress orientations from faults and calcite twins: a case study near the Sainte-Victoire Range (southern France). Tectonophysics 201, 141–156.

Lacombe, O., Angelier, J., Byrne, D., Dupin, J.-M., 1993. Eocene–Oligocene tectonics and kinematics of the Rhine–Saône continental transform zone (Eastern France). Tectonics 12, 874–888.

Larroque, J.-M., 1987. Analyse de la déformation de la série salifère du basin potassique de Mulhouse, et évolution du champ de contraintes dans le sud du fossé rhénan au teriaire et à l'actuel. Unpublished PhD Thesis, Univ. des sciences et techniques du Languedoc, Montpellier, 206 pp.

Larroque, J.-M., Ansart, M., 1984. Etude des fentes d'extension liées à la tectonique distensive du bassin potassique de Mulhouse. C. R. Acad. Sci. Paris 229, 1419–1424.

Larroque, J.M., Laurent, P., 1988. Evolution of the stress field pattern in the south of the Rhine Graben from the Eocene to present. Tectonophysics 148, 41–58.

Laubscher, H.P., 1961. Die Fernschubhypothese der Jurafaltung. Eclogae Geol. Helv. 54, 221–281.

Laubscher, H.P., 1972. Some overall aspect of the Jura dynamics. Am. J. Sci. 272, 293–304.

Laubscher, H.P., 1973. Jura Mountains. In: De Jong, K.A., Sholten, R. (Eds.), Gravity and Tectonics. Wiley, New York, pp. 217–227.

Laubscher, H.P., 1986. The eastern Jura: relations between thin-skinned and basement tectonics, local and regional. Geol. Rundsch. 75, 535–553.

Laubscher, H.P., 1992. Jura kinematics and the Molasse basin. Eclogae Geol. Helv. 85, 653–675.

Le Pichon, X., Bergerat, F., Roulet, M.-J., 1988. Plate kinematics and tectonics leading to Alpine belt formation: a new analysis. Processes in Continental Lithospheric Deformation. Geol. Soc. Am. Spec. Pap. 218, 111–131.

Letouzey, J., Colletta, B., Philippe, Y., 1995. Thrust propagation experimental models. AAPG International Conference and Exhibiting. AAPG Bull., vol. 75, 1204, abstracts.

Malavieille, J., 1984. Modélisation expérimentale des chevauchements imbriqués: application aux chaines de montagnes. Bull. Soc. Geol. Fr. 7, 129–138.

Marshak, S., Wilkerson, M.S., Hsui, A.T., 1992. Generation of curved fold-and-thrust belts; insight from simple physical and analytical models. In: Mc Clay, K.R. (Ed.), Thrust Tectonics. Chapman & Hall, London, pp. 83–92.

Martin, J., Mercier, E., 1994. L'accommodation locale: une solution alternative au problème de la conjonction des plans de kinks dans l'équilibrage d'une coupre (exemple dans le Jura externe). C. R. Acad. Sci. Paris 318, 1111–1115.

Martin, J., Mercier, E., 1996. Héritage distensif et structuration chevauchante dans une chaîne de couverture: apport de l'équilibrage par modélisation géométrique dans le Jura nord-occidental. Bull. Soc. Geol. Fr. 167, 101–110.

Mathis, M., 1974. La chaîne de l'Euthe (Jura). Unpublished Thesis, Univ. Besançon, 212 pp.

Mattauer, M., Mercier, J.-L., 1980. Microtectonique et grande tectonique. Mem. Hors-Ser. - Soc. Geol. Fr. 10, 141–161.

Mercier, J., Delibassis, N., Gauthier, A., Jarrige, J.J., Lemeille, F., Philip, H., Sebrier, M., Sorel, D., 1979. La néotectonic de l'arc égen. Rev. Geol. Dyn. Geogr. Phys. 21, 67–92.

Michel, P., Appert, G., Lavigne, J., Levavrais, A., Bonte, A., Lienhart, G., Ricour, J., 1953. Le contact Jura-Bresse dans la région de Lons-le-Saulnier. Bull. Soc. Geol. Fr., 3593–3611.

Mugnier, J.-L., Vialon, P., 1986. Deformation and displacement of the Jura cover on its basement. J. Struct. Geol. 8, 373–387.

Pavoni, N., 1980. Crustal stresses inferred from fault-plane solutions of earthquakes and neotectonic deformation in Switzerland. Rock Mech., Suppl. 9, 63–68.

Petit, J.-P., Mattauer, M., 1995. Paleostress superimposition deduced from mesoscale structures in limestones: the matelles exposure, Languedoc, France. J. Struct. Geol. 17, 245–256.

Philippe, Y., 1995. Rampes latérales et zones de transfert dans les chaînes plissées: géométrie, conditions de formation et pièges structuraux associés. Unpublished PhD Thesis, Univ. de Savoie, Grenoble, 257 pp.

Philippe, Y., Colletta, B., Deville, E., Mascle, A., Tardy, M., 1994. Transfer zone in the southern Jura thurst belt (eastern France): geometry, development and comparison with analogue modelling experiments. In: Mascle, A. (Ed.), Hydrocarbon and Petroleum Geology of France. Special Publication, vol. 4. European Association of Petroleum Geologists, Springer, Berlin, pp. 327–346.

Philippe, Y., Colletta, B., Deville, E., Mascle, A., 1996. The Jura fold-and-thrust belt: a kinematic model based on map-balancing. In: Ziegler, P.A., Horvath, F. (Eds.), Structure and Prospects of Alpine basins and forelands. Peri-Tethys Memoir 2, Edition du Muséum d'Histoire Naturelle, Paris, vol. 170, pp. 235–261.

Plessmann, W., 1972. Horizontal stylolithen im französich-schweizerischen Tafel und Faltenjura und ihre einpassung in den regionalen rahmen. Geol. Rundsch. 61, 332–347.

Rawnsley, K.D., Rives, T., Petit, J.P., 1992. Joint development in perturbed stress fields near faults. J. Struct. Geol. 14, 939–951.

Rebaï, S., Philip, H., Taboada, A., 1992. Modern tectonic stress field in the Mediterranean region: evidence for variation in stress directions at different scales. Geophys. J. Int. 110, 106–140.

Rocher, M., Lacombe, O., Angelier, J., Deffontaines, B., Verdier, F., 2000. Cenozoic folding and faulting in the south Aquitaine Basin (France): insights from combined structural and paleostress analyses. J. Struct. Geol. 22, 627–645.

Sassi, W., Colletta, B., Balé, P., Paquereau, T., 1993. Modeling of structural complexity in sedimentary basins: the role of pre-existing faults in thrust tectonics. Tectonophysics 226, 97–112.

Sissingh, W., 1998. Comparative tertiary stratigraphy of the Rhine Graben, Bresse Graben and Molasse Bassin: correlation of the Alpine foreland events. Tectonophysics 300, 249–284.

Sopena, J.P., Soulas, J.P., 1973. Etudes microtectoniques dans le Jura. Déformations des calcaires sous contrainte tectonique; essai d'interprétation et de corrélation des résultats pour l'ensemble de la chaîne: Unpublished Thesis, Univ. Besançon, France, 154 pp.

Tempier, C., 1987. Modèle nouveau de mise en place des structures provençales. Bull. Soc. Geol. Fr. 8, 533–540.

Tschanz, X., 1990. Analyse de la déformation du Jura central entre Neuchâtel (Suisse) et Besançon. Eclogae Geol. Helv. 83, 543–558.

Tschanz, X., Sommarugua, A., 1993. Deformation associated with folding above frontal and oblique ramps around the rhomb shaped Val-de-Ruz basin (Jura mountains). Ann. Tecton. 7, 53–70.

Vanbrabant, Y., Jongmans, D., Hassani, R., Bellino, D., 1999. An application o two-dimensional fnite-element modeling for studying the deformation of the Vraiscan fold-and-thrust belt (Belgium). Tectonophysics 309, 141–159.

Vialon, P., Bonnet, J.-L., Gamond, J.-F., Mugnier, J.-L., 1984. Modélisation des déformations d'une série stratifiée par le déplacement horizontal d'un poinçon. Application au Jura. Bull. Soc. Geol. Fr. 7, 139–150.

Villemin, T., 1987. L'évolution structurale du fossé rhénan au cours du Cénozoïque: un bilan de la déformation et des effets thermiques de l'extension. Bull. Soc. Geol. Fr. 8, 245–255.

Zoback, M.L., Zoback, M.D., Adams, J., Assumppçao, M., Bell, S., Bergman, E.A., Blümling, P., Brereton, N.R., Denham, D., Ding, J., Fichs, K., Gay, N., Gregersen, S., Gupta, H.K., Gvishinani, A., Jacob, K., Klein, R., Knoll, P., Magee, M., Mercier, J.L., Müller, B.C., Paquin, C., Rajendran, K., Stephansson, O., Suarez, G., Suter, M., Udias, A., Xu, Z.H., Zhizhin, M., 1989. Global pattern of tectonics stress. Nature 341, 291–298.